Journal of Orthopaedic Translation (2018) 15, 104—111

Available online at www.sciencedirect.com

ScienceDirect

journal homepage: http://ees.elsevier.com/jot

ORIGINAL ARTICLE

Disc degeneration promotes regional inhomogeneity in the trabecular morphology of loaded rat tail vertebrae

Li Ni ☆, Linlin Zhang ☆, Wei Xia, Guangdong Chen, Xudong Cui, Wen Zhang, Zongping Luo **, Huilin Yang*

Department of Orthopaedics, Orthopaedic Institute, The First Affiliated Hospital of SooChow University, China

Received 30 April 2018; received in revised form 22 July 2018; accepted 27 July 2018
Available online 22 August 2018

KEYWORDS
Animal model;
Disc degeneration;
Regional inhomogeneity;
Trabecular morphology

Summary *Background:* There is a close relationship between the vertebral trabecular morphology and the condition of the associated disc.
Objective: The relationship between disc degeneration and vertebral trabecular inhomogeneity is unclear. This study aimed to analyse the regional changes of vertebral trabecular morphology after disc degeneration.
Methods: Thirty male Sprague—Dawley rats were randomly assigned to five groups. Group 1 served as an experimental group for the assessment of disc degeneration induced by needle puncture. Group 2 served as a sham group for trabecular morphology analysis. In Group 3, rats had their tail bent between the eighth and tenth coccygeal vertebrae. In Group 4, the tail of rats was bent with a compression load of 4.5 N. In Group 5, rats first underwent disc degeneration induced by a needle puncture before their tail was bent with a compressive load of 4.5 N. Magnetic resonance imaging was performed on all groups, and histological examination was performed on rodents from Group 1. The ninth coccygeal vertebrae of rats from Groups 2—5 were scanned by Micro-computed tomography. Trabecular morphologic changes were assessed in the concave and convex regions by bone volume fraction, trabecular number, trabecular thickness and trabecular separation.
Results: Vertebral trabecular morphology in the concave region improved significantly, whereas the convex region was of significantly lower trabecular morphologic parameters with disc degeneration. The difference in trabecular morphologic parameters between the convex and concave regions increased significantly after disc degeneration.
Conclusion: Disc degeneration promotes regional inhomogeneity in the vertebral trabecular morphology, with the convex region of the vertebrae having the worse trabecular bone morphology than the concave region.

* Corresponding author.
** Corresponding author. Orthopaedic Institute of SooChow University, 708 Renmin Road, SuZhou, Jiangsu, 215007, China.
E-mail addresses: zongpingluo@suda.edu.cn (Z. Luo), hlyang@suda.edu.cn (H. Yang).
☆ These two authors contributed equally to this work.

https://doi.org/10.1016/j.jot.2018.07.008

The translational potential of this article: Our study indicates that disc degeneration promotes regional inhomogeneity in the vertebral trabecular morphology. Regional variations in trabecular microarchitecture are helpful to predict vertebral fragility. This may help to elucidate the mechanisms by which disc degeneration contributes to vertebral fracture.

Introduction

It is well documented that there is a close relationship between the disorganisation of the intervertebral disc and the changes seen in the trabecular bone architecture of the adjoining vertebral bodies [1,2]. With ageing, intervertebral discs tend to show progressive degenerative changes, which make them more fibrous and less able to evenly distribute compressive stress [3]. The trabecular bone adjacent to the vertebral endplates could then adapt to the altered force distribution in accordance with Wolff's law, resulting in the variations observed in bone architecture [4,5]. The vertebra-disc interaction can be viewed as a remodelling process in an attempt of the spinal segment to adapt to an altered biomechanical environment [6].

The relationship between disc degeneration and a higher vertebral fracture risk has been previously reported [7—9]. However, the relationship between disc degeneration and vertebral trabecular inhomogeneity is still controversial [7,10—12]. Although severe disc degeneration has been reported to transfer compressive load-bearing to the neural arch and reduce the trabecular architecture anteriorly [13], other authors showed that disc degeneration tended to be associated with greater trabecular bone volume fraction in the vertebral anterior region [10]. The problems underlying these inconsistent findings may lie in the complex relationships between age, disc degeneration and mechanical environment.

Therefore, the goal of this study was to develop an animal model in which the mechanical environment was controlled to investigate the single relationship between disc degeneration and regional trabecular morphologic changes. We hypothesised that disc degeneration could promote regional inhomogeneity in the vertebral trabecular morphology.

Materials and methods

Ethics statement

In this research, ethical approval was obtained from the animal experiment ethics committee of the investigator's institution (protocol number: 20160105-010). Both the Guide for the Care and Use of Laboratory Animal (1996) [14] and the ARRIVE (Animals in Research: Reporting In Vivo Experiments) guidelines [15] were followed.

Experimental samples

Thirty 12-week-old male Sprague—Dawley rats, weighing between 430 and 490 g, were used in this experiment and randomly assigned to one of the five following groups. In Group 1, rats were used for an assessment of disc degeneration induced by needle puncture (Co8-9 and Co9-10, $n = 6$). Group 2 served as a sham group ($n = 6$). In Group 3, rats were instrumented with an external device that bent the spine between the eighth and the tenth coccygeal vertebrae ($n = 6$). In Group 4, rats were instrumented with a compressive load of 4.5 N ($n = 6$). In Group 5, rats were instrumented with a compressive load of 4.5 N after undergoing disc degeneration of Co8-9 and Co9-10 induced by needle puncture ($n = 6$).

Surgical procedure

Needle puncture disc degeneration

Rats assigned to Groups 1 and 5 were anaesthetised with intraperitoneal injection of 1% pentobarbital sodium (40 mg/kg). The rat tails were cleaned with 70% ethanol, the vertebrae were palpated and the skin area corresponding to the intervertebral disc spaces between the eighth and the tenth coccygeal vertebrae was marked. An 18-gauge needle was inserted in the coronal plane at the levels of the annulus fibrosus of Co8-9 (proximal) and Co9-10 (distal), crossing the nucleus pulposus up to the contralateral annulus fibrosus (Figure 1A—B).

Load application

Seven days after the needle puncture, rats assigned to Groups 3—5 were anaesthetised. Rat tails were cleaned again and then instrumented with an external device. Two K-wires (length: 50 mm; diameter: 1.2 mm) were inserted percutaneously into the vertebrae adjacent to the Co8-9 and Co9-10 discs. Two wires were fixed at a 40° angle on the concave side of the bending of the tail. Tension springs were placed 25 mm away from the axis centre of the tail with a 4.5-N loading. A plastic plate was used to prevent vertebrae torsion on the dorsum of the tail (Figure 1C—D).

Measurement of disc degeneration

Magnetic resonance imaging

Magnetic resonance imaging (MRI) was performed on Group 1 7 days after needle puncture and on Groups 2—5 14 days after loading, using a 1.5-T system (General Electric Company, Chicago, USA). Imaging sequences included spin-echo T2-weighted images (repletion time: 3000 ms; echo time:

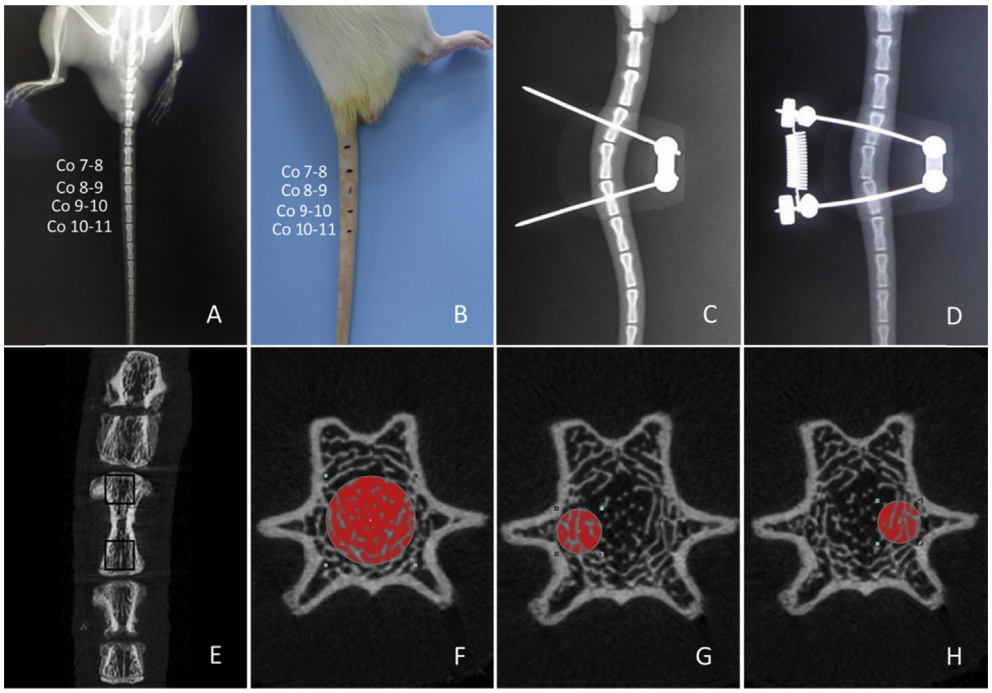

Figure 1 (A) Disc location of rat tail under X-ray fluoroscopy; (B) needle puncturing in the coronal plane at the Co8-9 and Co9-10 levels; (C) Two K-wires were fixed at a 40° angle on the concave side of the bending of the tail; (D) A tension spring with 4.5-N loading was placed on the convex side of the bending of the tail; (E) The trabecular bone structures in the proximal and distal ends of the ninth coccygeal vertebral body were analysed; (F) the global region of interest for assessing the trabecular bone structure; (G) The convex region of interest for assessing the trabecular bone structure; (H) the concave region of interest for assessing the trabecular bone structure.

80 ms; field of view: 200 mm × 200 mm; slice thickness: 1.4 mm) in the coronal plane. Disc images were classified into five grades using the Pfirrmann classification by four blinded researchers [16].

Histological analysis

After the completion of MRI scanning, Group 1 rats were euthanised by an overdose of an anaesthetic. The target discs Co8-9 and Co9-10 and adjacent discs Co7-8 and Co10-11 were dissected from the skin and soft tissues. Discs were fixed in a 10% buffered formalin solution for 24 h and decalcified in 10% ethylenediaminetetraacetic acid for 30 days, then paraffin-embedded and finally sectioned with a 5-μm thickness. The sections were stained with hematoxylin/eosin, safranin O/Fast green and Mallory stain for histological score. Images were obtained using the Axio Imager (Carl Zeiss, Jena, Germany). Four blinded researchers graded the sections using the Norcross classification [10 (nondegenerated) to 2 (severely degenerated)] [17].

Measurement of trabecular morphology

After 14 days of loading, the ninth coccygeal vertebrae of rats assigned to Groups 2—5 were scanned using Micro-computed tomography (SkyScan 1176; Bruker-microCT, Kontich, Belgium). The scanning conditions remained identical for all the tests (18 μm, 65 kV, 380 μA, 1-mm Al filter, 600-ms exposure). The regions of interest (diameter: 2.2 mm) were strictly placed in the proximal and distal trabecular bone structure of the ninth coccygeal vertebral body. Both the proximal and distal regions were further divided into a convex region and a concave region (diameter: 1.1 mm) (Figure 1E—H). Image segmentation into a bone and bone marrow phase was obtained by applying a fixed threshold for all samples. The following three-dimensional indices describing the trabecular bone morphology were assessed: bone volume fraction (BV/TV), trabecular number (Tb.N), trabecular thickness (Tb.Th) and trabecular separation (Tb.Sp). The regional trabecular morphologic changes between different groups were compared.

Statistical analysis

Data are expressed as mean ± standard deviation. All statistical analyses were performed using StatView (SAS Institute, Cary, NC, USA), with the level of significance being set at $p < 0.05$. For disc MRI and histological grades with needle puncture, a Wilcoxon rank-sum test was used to determine whether the puncture level (Co8-9 and Co9-10) differed from the control level (Co7-8 and Co10-11) in Group 1. For disc degeneration MRI grades and the trabecular bone morphologic data, Kruskal—Wallis tests were used to detect potential significant differences between Groups 2—5.

Results

Assessment of disc degeneration

A significant difference was observed in T2-weighted MRI images after 7 days of needle puncture and 14 days of loading ($p < 0.05$, Figure 2). The histological scores were significantly lower for the needle puncture discs than for the control discs ($p < 0.05$, Figure 3A). Histological results revealed nucleus dehydration with more fibrosis and annular disorganisation after needle puncture (Figure 4A—F).

Measurement of trabecular morphology

The disc degeneration induced in Group 5 resulted in a significant increase in BV/TV, Tb.N and Tb.Th accompanied by a decrease of Tb.Sp when compared with Group 4 ($p < 0.05$, Figure 5). The trabecular morphology improved significantly in the concave region of Group 5, whereas the convex region was of significantly worse trabecular bone morphology ($p < 0.05$, Figure 6). The difference in trabecular morphologic parameters between the convex and concave regions increased significantly after disc degeneration ($p < 0.05$, Figures 7 and 8).

Discussion

We have developed an *in vivo* rat tail model in which the relationship between disc degeneration and regional trabecular morphologic changes can be illustrated. In this study, our most notable findings were that disc degeneration promoted regional inhomogeneity in the vertebral trabecular morphology (See Tables 1 and 2).

Rat tail disc has been validated as a suitable model of the human disc regarding geometry and axial mechanics [18—20]. Stab injury has been reported to create rapid histological changes in rat tail discs [21—23]. Nuclear size decrease and annular layer disorganisation are consistent with human degenerative discs [24—26]. We observed morphologic changes in rat tail discs 7 days after needle puncture. With MRI, needle puncture—induced discs exhibited an inhomogeneous structure with a loss of intranuclear T2 hyperintensity. Histological sections indicated nuclear depressurisation, annulus layer disorganisation, inner annulus inward bulging and radial annular tears. These degenerative changes are similar to those described for human disc degeneration [24,27]. The human intervertebral disc is always under complex load [28]. This load arises partly from the body weight and partly from the muscle and the ligament tensions [29]. After disc degeneration, the rat tails were bent at 40° and loaded with 4.5 N to simulate the human lumbar intervertebral disc angle and loading [30,31]. As the posterior region is the path through which some axial stress is transferred to the neural arches, this region receive more stress than the anterior region, resulting in a better bone structure posteriorly [32,33]. We observed that the concave region of the coccygeal vertebrae was of significantly better trabecular bone morphology than the convex region after bending and compression. These findings suggest that this model can be used to better understand the relationship between disc degeneration and vertebral trabecular morphologic changes.

Human vertebral trabeculae are not morphologically homogeneous. Banse et al [34] reported that BV/TV in the posterior region of lumbar vertebral body was 20% higher than in the anterior one. Hulme et al [32] found that the inferoposterior region had the highest BV/TV in the vertebral body. Vertebral trabecular architecture has been shown to be closely related to age and to the state of intervertebral discs [1,4,35,36]. A significant age-related decrease in trabecular quality has been reported in previous studies [37,38]. Age-related decrease in BV/TV and increase in Tb.N were more pronounced after the age of 70 years, with a rate of −6.4% and +4.9% per decade, respectively [35]. Decreases in trabecular BV/TV with age are similar in women and men [39]. However, the relationship between disc degeneration and trabecular architecture inhomogeneity is unclear. Most researchers agree that there is a negative linear relationship between disc health and trabecular structure [2,7], but Wang et al [10] found conflicting results. We investigated the relationship between disc degeneration and regional trabecular morphologic changes using an animal model. A positive

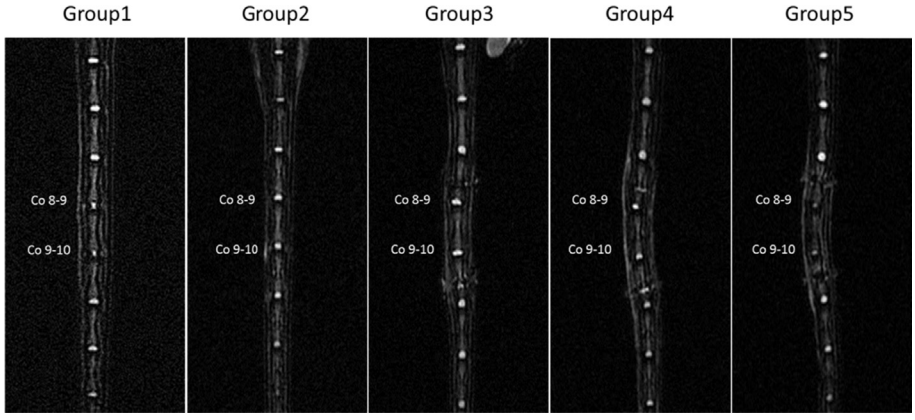

Figure 2 Magnetic resonance imaging was performed on rat tail 7 days after needle puncture on Group 1 and 14 days after loading on Groups 2—5. Needle-punctured discs exhibited an inhomogeneous structure with a loss of T2 hyperintensity in MRI on Group 1. After 14 days of loading, T2 hyperintensity was lost more severely on Group 5.
MRI = magnetic resonance imaging.

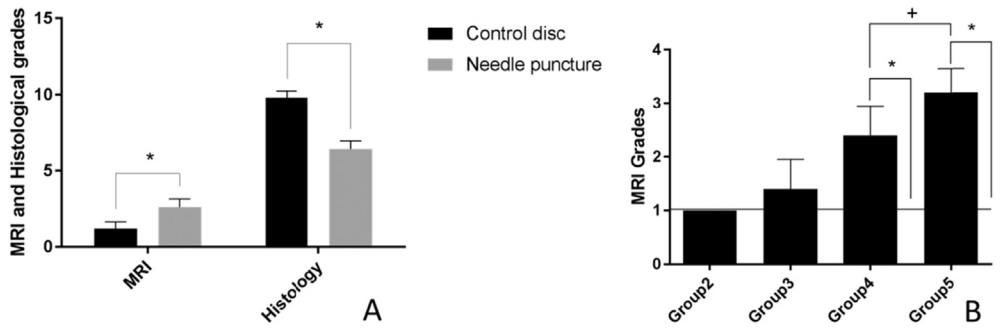

Figure 3 (A) The needle-punctured discs showed significantly higher degenerative scores according to Pfirrmann MRI classification, and the histological scores were significantly lower than those of the control discs defined by Norcross, $^{*}p < 0.05$; (B) After 14 days of loading, the needle-punctured discs on Group 5 showed significantly higher degenerative scores, $^{*,+}p < 0.05$.
MRI = magnetic resonance imaging.

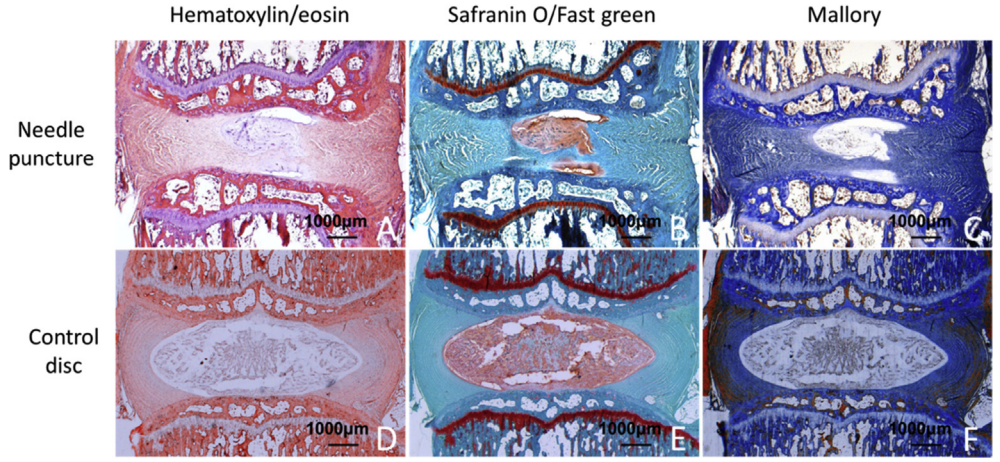

Figure 4 (A) Representative hematoxylin/eosin, (B) safranin O/Fast green (C) and Mallory staining images of a needle-punctured disc; (D–F) the same staining images of a control disc (original magnification ×25).

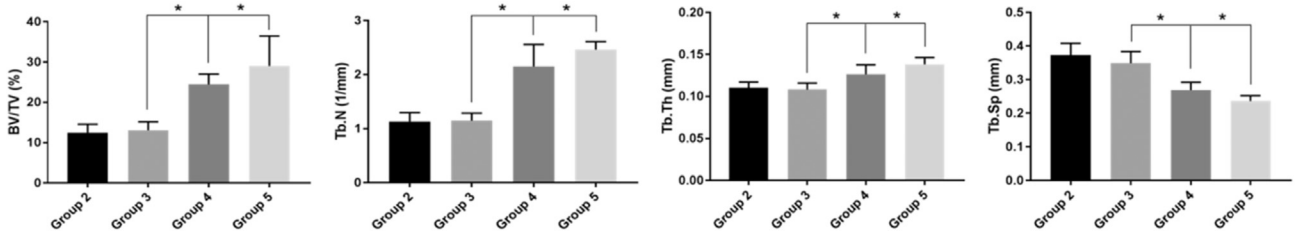

Figure 5 Trabecular parameters in Group 5 increased in BV/TV, Tb.N and Tb.Th accompanied by a decrease of Tb.Sp when compared with Group 4.
BV/TV = bone volume fraction; Tb.N = trabecular number; Tb.Sp = trabecular separation; Tb.Th = trabecular thickness.

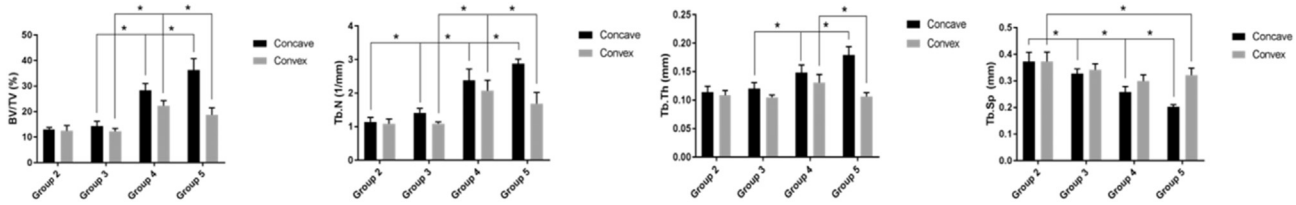

Figure 6 Trabecular parameters in the concave region of Group 5 improved significantly, whereas those of the convex region were significantly worse except Tb.Sp.
BV/TV = bone volume fraction; Tb.N = trabecular number; Tb.Sp = trabecular separation; Tb.Th = trabecular thickness.

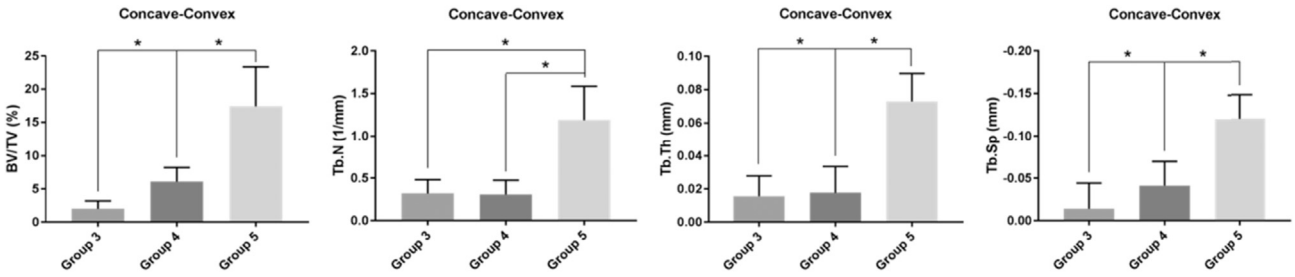

Figure 7 The difference in trabecular morphology parameters of Group 5 between the convex and concave regions increased significantly.
BV/TV = bone volume fraction; Tb.N = trabecular number; Tb.Sp = trabecular separation; Tb.Th = trabecular thickness.

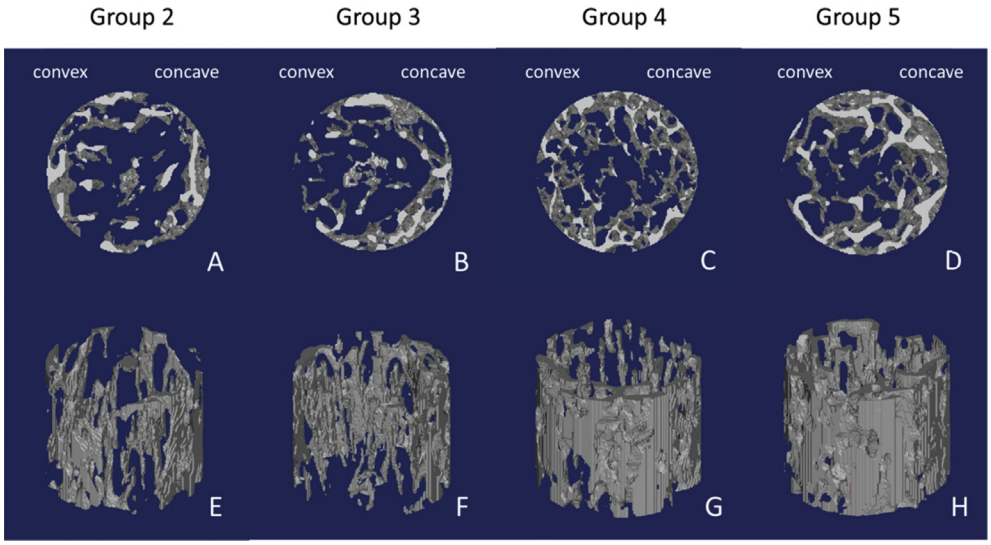

Figure 8 (A—D) Top view and (E—H) isometric view of the ninth coccygeal vertebral trabecular morphology from the centre of the vertebral body with diameter of 2.2 mm. The trabecular morphologic parameters improved significantly in the concave region, whereas those in the convex region were significantly worse after disc degeneration.

Table 1 Trabecular morphologic parameters in the global region of the vertebral body in Groups 2—5.

Parameters	Group 2	Group 3	Group 4	Group 5	χ^2	*P*
BV/TV (%)	12.48 ± 2.10	13.10 ± 2.08	24.46 ± 2.54	29.04 ± 7.40	29.66	<0.001
Tb.N (1/mm)	1.13 ± 0.16	1.15 ± 0.13	2.15 ± 0.40	2.46 ± 0.15	30.60	<0.001
Tb.Th (mm)	0.11 ± 0.01	0.11 ± 0.01	0.13 ± 0.02	0.14 ± 0.03	21.99	<0.001
Tb.Sp (mm)	0.37 ± 0.04	0.35 ± 0.03	0.27 ± 0.02	0.24 ± 0.02	32.42	<0.001

BV/TV = bone volume fraction; Tb.N = trabecular number; Tb.Sp = trabecular separation; Tb.Th = trabecular thickness.

relationship was found in the vertebral concave region, but a negative relationship was found in the convex region. The concave trabecular morphology in the disc degeneration group showed an increase in BV/TV, Tb.N and Tb.Th accompanied by a decrease in Tb.Sp, but the trabecular bone morphologic parameters in the convex region decreased significantly. With disc degeneration, the hydrostatic nucleus becomes smaller and decompressed, and more of the compressive load-bearing is supported by the concave annulus [40]. Trabecular bone adjacent to the vertebral endplates could then adapt to the altered force distribution. Consequently, the heterogeneity in trabecular morphology between the convex and concave regions increased significantly.

Understanding the relationships between disc degeneration and trabecular regional changes in the vertebral body may help to elucidate the mechanisms by which disc degeneration contributes to vertebral fracture. Previous *in vitro* studies have demonstrated that taking into account the trabecular architecture improves the prediction of vertebral strength [41]. Indeed, BV/TV in combination with microarchitecture and its heterogeneity improved the prediction of vertebral mechanical behaviour up to 86% of the variability in vertebral failure load [33]. Regional variations in trabecular microarchitecture are helpful to predict vertebral fragility [32].

Our study demonstrated that disc degeneration leads to secondary vertebral trabecular changes caused by

Table 2 Trabecular morphologic parameters in the concave and convex regions of the vertebral body in Groups 2–5.

Parameters	Region	Group 2	Group 3	Group 4	Group 5	χ^2	*P*
BV/TV (%)	Concave	12.98 ± 0.85	14.32 ± 1.90	28.36 ± 2.65	36.21 ± 4.53	33.01	<0.001
	Convex	12.48 ± 2.10	12.30 ± 1.12	22.26 ± 1.99	18.71 ± 2.78	30.48	<0.001
	Concave-convex		2.02 ± 1.18	6.10 ± 2.13	17.50 ± 5.93	25.32	<0.001
Tb.N (1/mm)	Concave	1.14 ± 0.13	1.41 ± 0.14	2.38 ± 0.33	2.87 ± 0.14	34.81	<0.001
	Convex	1.09 ± 0.14	1.09 ± 0.05	2.07 ± 0.31	1.68 ± 0.34	29.45	<0.001
	Concave-convex		0.32 ± 0.16	0.31 ± 0.17	1.19 ± 0.40	19.42	<0.001
Tb.Th (mm)	Concave	0.11 ± 0.01	0.12 ± 0.01	0.15 ± 0.01	0.18 ± 0.01	31.30	<0.001
	Convex	0.11 ± 0.01	0.10 ± 0.02	0.13 ± 0.01	0.11 ± 0.01	19.27	<0.001
	Concave-convex		0.01 ± 0.01	0.02 ± 0.01	0.07 ± 0.02	19.44	<0.001
Tb.Sp (mm)	Concave	0.37 ± 0.03	0.33 ± 0.02	0.26 ± 0.02	0.22 ± 0.01	35.60	<0.001
	Convex	0.37 ± 0.04	0.34 ± 0.02	0.30 ± 0.02	0.32 ± 0.03	22.38	<0.001
	Concave-convex		−0.01 ± 0.03	−0.04 ± 0.02	−0.12 ± 0.03	21.08	<0.001

BV/TV = bone volume fraction; Tb.N = trabecular number; Tb.Sp = trabecular separation; Tb.Th = trabecular thickness.

remodelling, which was stimulated by the changes in the biomechanical environment. Vertebral trabecular inhomogeneity is influenced not only by age but also by disc degeneration. However, this study had several limitations. First, the relationship between disc degeneration and trabecular morphologic changes was described in a static mechanical environment. The human intervertebral disc is responsible for carrying dynamic compressive loading while maintaining flexibility in different body postures. Therefore, the relationship between disc degeneration and regional trabecular morphologic changes may be more applicable to human lumbar spine in the upright posture. Second, the load applied on the human disc is mainly compressive, but it is also subjected to other types of loads such as tensile and shear stresses [42]. In our model, only axial compression was applied. Third, severe disc degeneration with load-bearing by the neural arch could not be simulated. Severely degenerated discs typically lose height, causing the anterior vertebral body to be stress shielded, thus leading to bone loss [7]. Despite these limitations, this model truly mimics the vertebral trabecular morphologic changes adapting to the disc degeneration in the remodelling process. In the future, the regional trabecular morphologic changes after disc degeneration need to be analysed under intermittent dynamic mechanical environment.

In conclusion, disc degeneration promotes regional inhomogeneity in the vertebral trabecular morphology. The convex region of the vertebrae has the worse trabecular bone morphology than the concave region.

Conflicts of interest

All authors declare that they have no conflict of interest.

Acknowledgements

This work was supported by the National Natural Science Foundation of China (81320108018, 31570943 and 31270995), Innovation and Entrepreneurship Program of Jiangsu Province, Jiangsu Provincial Special Program of Medical Science (BL2012004) and the Priority Academic Program Development of Jiangsu Higher Education Institutions.

Appendix A. Supplementary data

Supplementary data related to this article can be found at https://doi.org/10.1016/j.jot.2018.07.008.

References

[1] Simpson EK, Parkinson IH, Manthey B, Fazzalari NL. Intervertebral disc disorganization is related to trabecular bone architecture in the lumbar spine. J Bone Miner Res 2001;16(4):681–7.
[2] Hussein AI, Jackman TM, Morgan SR, Barest GD, Morgan EF. The intravertebral distribution of bone density: correspondence to intervertebral disc health and implications for vertebral strength. Osteoporosis Int 2013;24(12):3021–30.
[3] Adams MA, Roughley PJ. What is intervertebral disc degeneration, and what causes it? Spine 2006;31(18):2151–61.
[4] Adams MA, McNally DS, Dolan P. 'Stress' distributions inside intervertebral discs - the effects of age and degeneration. J Bone Joint Surg Br 1996;78b(6):965–72.
[5] Pollintine P, Dolan P, Tobias JH, Adams MA. Intervertebral disc degeneration can lead to "stress-shielding" of the anterior vertebral body - a cause of osteoporotic vertebral fracture? Spine 2004;29(7):774–82.
[6] Moore RJ, Vernon-Roberts B, Osti OL, Fraser RD. Remodeling of vertebral bone after outer anular injury in sheep. Spine (Phila Pa 1976) 1996;21(8):936–40.
[7] Adams MA, Pollintine P, Tobias JH, Wakley GK, Dolan P. Intervertebral disc degeneration can predispose to anterior vertebral fractures in the thoracolumbar spine. J Bone Miner Res 2006;21(9):1409–16.
[8] Sornay-Rendu E, Allard C, Munoz F, Duboeuf F, Delmas PD. Disc space narrowing as a new risk factor for vertebral fracture - the OFELY study. Arthritis Rheum 2006;54(4):1262–9.
[9] Castano-Betancourt MC, Oei L, Rivadeneira F, de Schepper EI, Hofman A, Bierma-Zeinstra S, et al. Association of lumbar disc degeneration with osteoporotic fractures; the Rotterdam study and meta-analysis from systematic review. Bone 2013;57(1):284–9.
[10] Wang Y, Owoc JS, Boyd SK, Videman T, Battie MC. Regional variations in trabecular architecture of the lumbar vertebra:

associations with age, disc degeneration and disc space narrowing. Bone 2013;56(2):249—54.
[11] Adams M, Dolan P. Vertebral fracture and intervertebral discs. J Bone Miner Res 2012;27(6). 1432-32.
[12] Wang Y, Boyd S, Battie M, Yasui Y, Videman T. Response to "Vertebral fracture and intervertebral discs". J Bone Miner Res 2012;27(6):1433—4.
[13] Pollintine P, Przybyla AS, Dolan P, Adams MA. Neural arch load-bearing in old and degenerated spines. J Biomech 2004; 37(2):197—204.
[14] Resources IoLA. Guide for the care and used of laboratory animals. National Academies Press; 1996.
[15] Kilkenny C, Browne WJ, Cuthill IC, Emerson M, Altman DG. Improving bioscience research reporting: the ARRIVE guidelines for reporting animal research. PLoS Biol 2010;8(6). e1000412.
[16] Pfirrmann CW, Metzdorf A, Zanetti M, Hodler J, Boos N. Magnetic resonance classification of lumbar intervertebral disc degeneration. Spine (Phila Pa 1976) 2001;26(17):1873—8.
[17] Norcross JP, Lester GE, Weinhold P, Dahners LE. An in vivo model of degenerative disc disease. J Orthop Res: Official Publ Orthop Res Soc 2003;21(1):183—8.
[18] O'Connell GD, Vresilovic EJ, Elliott DM. Comparison of animals used in disc research to human lumbar disc geometry. Spine 2007;32(3):328—33.
[19] Elliott DM, Sarver JJ. Young investigator award winner: validation of the mouse and rat disc as mechanical models of the human lumbar disc. Spine 2004;29(7):713—22.
[20] Beckstein JC, Sen S, Schaer TP, Vresilovic EJ, Elliott DM. Comparison of animal discs used in disc research to human lumbar disc. Spine 2008;33(6):E166—73.
[21] Han B, Zhu K, Li FC, Xiao YX, Feng J, Shi ZL, et al. A simple disc degeneration model induced by percutaneous needle puncture in the rat tail. Spine 2008;33(18):1925—34.
[22] Zhang HN, La Marca F, Hollister SJ, Goldstein SA, Lin CY. Developing consistently reproducible intervertebral disc degeneration at rat caudal spine by using needle puncture laboratory investigation. J Neurosurg Spine 2009;10(6): 522—30.
[23] Zhang HN, Yang SS, Wang L, Park P, La Marca F, Hollister SJ, et al. Time course investigation of intervertebral disc degeneration produced by needle-stab injury of the rat caudal spine laboratory investigation. J Neurosurg Spine 2011;15(4): 404—13.
[24] Boos N, Weissbach S, Rohrbach H, Weiler C, Spratt KF, Nerlich AG. Classification of age-related changes in lumbar intervertebral discs. Spine 2002;27(23):2631—44.
[25] Rousseau MAA, Ulrich JA, Bass EC, Rodriguez AG, Liu JJ, Lotz JC. Stab incision for inducing intervertebral disc degeneration in the rat. Spine 2007;32(1):17—24.
[26] Issy AC, Castania V, Castania M, Salmon CEG, Nogueira-Barbosa MH, Del Bel E, et al. Experimental model of intervertebral disc degeneration by needle puncture in Wistar rats. Braz J Med Biol Res 2013;46(3):235—44.
[27] Thompson JP, Pearce RH, Schechter MT, Adams ME, Tsang IK, Bishop PB. Preliminary evaluation of a scheme for grading the gross morphology of the human intervertebral disc. Spine (Phila Pa 1976) 1990;15(5):411—5.
[28] Inoue N, Espinoza Orías AA. Biomechanics of intervertebral disk degeneration. Orthop Clin N Am 2011;42(4):487—99.
[29] Neidlinger-Wilke C, Galbusera F, Pratsinis H, Mavrogonatou E, Mietsch A, Kletsas D, et al. Mechanical loading of the intervertebral disc: from the macroscopic to the cellular level. Eur Spine J: Official Publication of the European Spine Society, the European Spinal Deformity Society, and the European Section of the Cervical Spine Research Society 2014;23(Suppl 3): S333—43.
[30] Court C, Colliou OK, Chin JR, Liebenberg E, Bradford DS, Lotz JC. The effect of static in vivo bending on the murine intervertebral disc. Spine J 2001;1(4):239—45.
[31] Iatridis JC, Mente PL, Stokes IA, Aronsson DD, Alini M. Compression-induced changes in intervertebral disc properties in a rat tail model. Spine (Phila Pa 1976) 1999;24(10): 996—1002.
[32] Hulme PA, Boyd SK, Ferguson SJ. Regional variation in vertebral bone morphology and its contribution to vertebral fracture strength. Bone 2007;41(6):946—57.
[33] Wegrzyn J, Roux JP, Arlot ME, Boutroy S, Vilayphiou N, Guyen O, et al. Role of trabecular microarchitecture and its heterogeneity parameters in the mechanical behavior of ex vivo human L-3 vertebrae. J Bone Miner Res 2010;25(11): 2324—31.
[34] Banse X, Devogelaer JP, Munting E, Delloye C, Cornu O, Grynpas M. Inhomogeneity of human vertebral cancellous bone: systematic density and structure patterns inside the vertebral body. Bone 2001;28(5):563—71.
[35] Stauber M, Muller R. Age-related changes in trabecular bone microstructures: global and local morphometry. Osteoporosis Int 2006;17(4):616—26.
[36] Thomsen JS, Niklassen AS, Ebbesen EN, Bruel A. Age-related changes of vertical and horizontal lumbar vertebral trabecular 3D bone microstructure is different in women and men. Bone 2013;57(1):47—55.
[37] Gong H, Zhang M, Yeung HY, Qin L. Regional variations in microstructural properties of vertebral trabeculae with aging. J Bone Miner Metabol 2005;23(2):174—80.
[38] Chen HY, Zhou XR, Fujita H, Onozuka M, Kubo KY. Age-related changes in trabecular and cortical bone microstructure. Internet J Endocrinol 2013;2013, 213234.
[39] Chen H, Shoumura S, Emura S, Bunai Y. Regional variations of vertebral trabecular bone microstructure with age and gender. Osteoporos Int 2008;19(10):1473—83.
[40] Galbusera F, van Rijsbergen M, Ito K, Huyghe JM, Brayda-Bruno M, Wilke HJ. Ageing and degenerative changes of the intervertebral disc and their impact on spinal flexibility. Eur Spine J: Official publication of the European Spine Society, the European Spinal Deformity Society, and the European Section of the Cervical Spine Research Society 2014;23(Suppl 3): S324—32.
[41] Fields AJ, Eswaran SK, Jekir MG, Keaveny TM. Role of trabecular microarchitecture in whole-vertebral body biomechanical behavior. J Bone Miner Res 2009;24(9): 1523—30.
[42] Stokes IAF, Iatridis JC. Mechanical conditions that accelerate intervertebral disc degeneration: overload versus immobilization. Spine 2004;29(23):2724—32.